Systematic study of charge-state and energy dependences of transfer-ionization to single-electron-capture ratios for F^{q+} ions incident on He

R. Ünal,* P. Richard, I. Ben-Itzhak,† C. L. Cocke, M. J. Singh,‡ H. Tawara,§ and N. Woody
J.R. Macdonald Laboratory, Department of Physics, Kansas State University, Manhattan, Kansas 66506, USA
(Received 7 March 2007; published 17 July 2007)

This paper presents an investigation of the charge-state and energy dependences of transfer-ionization (TI) and single-electron-capture (SC) processes for fluorine ions ($q=4+$ to $9+$) incident on a supersonic He jet target. The measurements were made for beam energies between 0.5 and 2.5 MeV/u. A recoil ion momentum spectrometer was used to separate TI and SC based on the longitudinal momentum transfer and time of flight of the recoil ions. The cross-section ratios for TI to SC, $R=\sigma_{TI}/\sigma_{SC}$, were determined and observed to decrease monotonically with velocity. The values of R were combined with measured total transfer cross sections to deduce the cross sections for both SC and TI. Coupled-channel calculations of the energy dependence of TI and SC for $F^{9+}+He$ were compared to the experimental cross sections as well as the values of R. The calculated cross sections were found to be slightly lower and the R values slightly higher than the measured values, but with approximately the same energy dependences. A q^2 scaling of the $He^{2+}+He$ data was also compared to the present data and was found to give unexpected good agreement.

DOI: 10.1103/PhysRevA.76.012710 PACS number(s): 34.70.+e, 34.90.+q, 34.50.Fa

I. INTRODUCTION

Over the last few decades several investigators have studied single-capture (SC) and transfer-ionization (TI) processes both theoretically and experimentally in ion-atom collisions for fast, highly charged ions [1–4].

Collisions involving multiply charged ions and neutral atoms are characterized by the presence and simultaneous action of several collision channels, resulting in multielectron transitions within and between participating systems [5]. The classical trajectory Monte Carlo (CTMC) technique developed for handling many electron systems has been successful in describing the total cross sections and the momentum distributions of the scattered particles for a few systems [6]. Rigorous coupled-channel calculations for these types of systems are very difficult to perform because of the large basis set required to describe the final states of the reaction products and due to difficulties in obtaining the proper interaction potential for the multielectron projectiles and target atoms. Because of these difficulties, only a limited number of such calculations have been performed. Thus, it is important to provide the systematics of these processes from accurate experimental measurements to serve as a guide to theoretical calculations.

For two-electron target atoms the problem reduces to one- and two-electron processes. These processes can be specified as follows:

$$\begin{aligned} A^{q+}+He &\rightarrow A^{q+}+He^{+}+e^{-} \quad \text{SI—single ionization,}\\ &\rightarrow A^{(q-1)+}+He^{+} \quad \text{SC—single capture,}\\ &\rightarrow A^{(q-1)+}+He^{2+}+e^{-} \quad \text{TI—transfer ionization,}\\ &\rightarrow A^{q+}+He^{2+}+2e^{-} \quad \text{DI—double ionization,}\\ &\rightarrow A^{(q-2)+}+He^{2+} \quad \text{DC—double capture.} \end{aligned}$$

Many reviews of charge transfer have been published since the 1950s. The authors of some of the reviews are listed here: Massey and Burhop [7], Allison [8], Allison and Garcia-Munoz [9], Hasted [10], Betz [11], Tawara and Russek [12], Massey and Gilbody [13], Gilbody [14], and Bransden and McDowell [15].

The cross sections of TI and SC, for the collisions of fast highly charged ions with He, can be written in impact parameter space within the independent electron model, IEM, using the uncoupled ionization probability, $P_i(b)$, excitation probability, $P_{exc}(b)$, and capture probability, $P_c(b)$. The model assumes that each electron interacts independently with an effective potential of the projectile and not with each other. The probabilities for SI, DI, SC, and TI can be expressed in the IEM in terms of these probabilities as

$$\begin{aligned} P_{SI}(b) &= 2P_i(b)[1-P_i(b)-P_{exc}(b)-P_c(b)],\\ P_{DI}(b) &= P_i^2(b),\\ P_{SC}(b) &= 2P_c(b)[1-P_i(b)-P_{exc}(b)-P_c(b)],\\ P_{TI}(b) &= 2P_c(b)P_i(b). \end{aligned} \tag{1}$$

The cross section for SC and TI can then be written as

$$\begin{aligned} \sigma_{SC} &= 2\pi\int_0^\infty P_{SC}(b)bdb,\\ \sigma_{TI} &= 2\pi\int_0^\infty P_{TI}(b)bdb. \end{aligned} \tag{2}$$

Substitution of Eq. (1) into Eq. (2) yields

$$\sigma_{SC} = 2\pi\int_0^\infty 2P_c(b)[1-P_i(b)-P_{exc}(b)-P_c(b)]bdb,$$

*Present address: Afyon Kocatepe University, Afyon, Turkey.
†Corresponding author. ibi@phys.ksu.edu
‡Present address: The Institute for Plasma Research, Bhat Gandhinagar, India.
§Present address: Max Planck Institute for Nuclear Physics, Heidelberg, Germany.

$$\sigma_{TI} = 2\pi \int_0^\infty 2P_c(b)P_i(b)bdb. \tag{3}$$

One characteristic of these probabilities is that $P_i(b)$ and $P_{exc}(b)$ are approximately constant over the range of b where $P_c(b)$ is nonzero and strongly dependent on b. This leads to the following approximate result

$$R = \frac{\sigma_{TI}}{\sigma_{SC}} = \frac{2\pi 2P_i(b)\int_0^\infty P_c(b)bdb}{2\pi 2[1 - P_i(b) - P_{exc}(b)]\int_0^\infty P_c(b)bdb},$$

$$R \approx \frac{P_i(b)}{1 - P_i(b) - P_{exc}(b)} \approx \frac{P_i(b)}{1 - P_i(b)}, \tag{4}$$

where in the first step we also used the fact that for the fast collisions under consideration $P_c(b)$ is much smaller than $P_i(b)$ and $P_{exc}(b)$, while for the last step we took advantage of the fact that $P_{exc}(b)$ is also much smaller than $P_i(b)$.

Understanding collisions with bare projectiles is essential to proceed towards dressed projectiles. However, we cannot use the collision information from bare projectiles indiscriminately to predict the behavior of the dressed projectile. In this paper we present a systematic experimental study of both charge and energy dependence of dressed and bare projectiles.

II. EXPERIMENT

The measurements were performed in the J.R. Macdonald Laboratory at Kansas State University. Ion beams of interest were extracted from the EN tandem Van de Graaff accelerator, poststripped with either a carbon foil or gas stripper as required to obtain sufficient beam current and then momentum analyzed in order to obtain the desired charge-state beam on the gas target. The collision chamber is commissioned on the 15° port of a switching magnet. The switching magnet made a clear charge-state selection by eliminating undesirable contributions from beam contamination. The ion beam was monitored with beam profile monitors and Faraday cups along its path. Ion beam monitoring was especially useful in determining the ion beam passage through the gas jet target directed between two of the equipotential plates of the recoil ion spectrometer. The amount of beam was controlled by two sets of four-jaw slits and three apertures; one [outer diameter (o.d.)=5 mm] before the chamber and two (o.d.=5 and 3 mm) after the chamber. The charge exchange beam was selected with a dipole magnet after the collision chamber and directed to a scintillator attached to a photomultiplier tube located at a 9° offset from the beam line axis.

The target was provided by a supersonic He jet with a two-stage collimation as described in detail elsewhere [16,17]. Target recoil ions produced in projectile ion-He collisions were charge state analyzed using a two stage electrostatic time-of-flight spectrometer [16,17]. The recoil ions were extracted by the two static-electric field regions followed by a field-free region and detected with a chevron

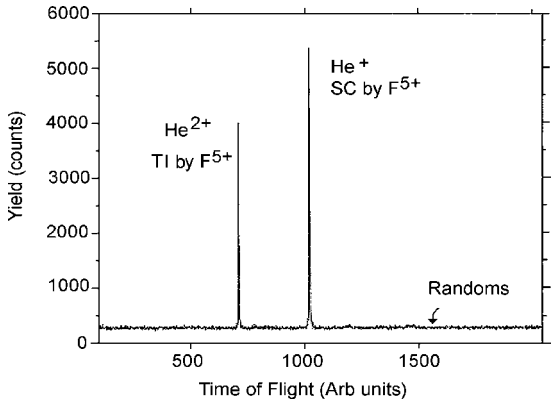

FIG. 1. Recoil ion time-of-flight (TOF) spectrum for 1.5 MeV/u F^{5+} on He. Note that both He^{n+} peaks are measured in coincidence with the emerging F^{4+} ions.

arrangement of microchannel plates coupled to a position sensitive resistive anode. Typical channel plate bias was 900 V across each plate. Recoil ion flight times are proportional to the square root of the mass-to-charge ratio of the ion. The dimensions of the spectrometer were designed to allow for approximate first order time focusing of recoil ions produced at different positions in the extraction region. The first order time focusing condition was satisfied for the static electric field-free drift length that is approximately twice the distance from the beam to the field-free region. Recoil ion flight times were in the range of 2.6 and 3.6 μs for He^{2+} and He^{+}, respectively, for an extraction voltage of 1500 V on the pusher plate and 852 V on the focusing plate of the spec-

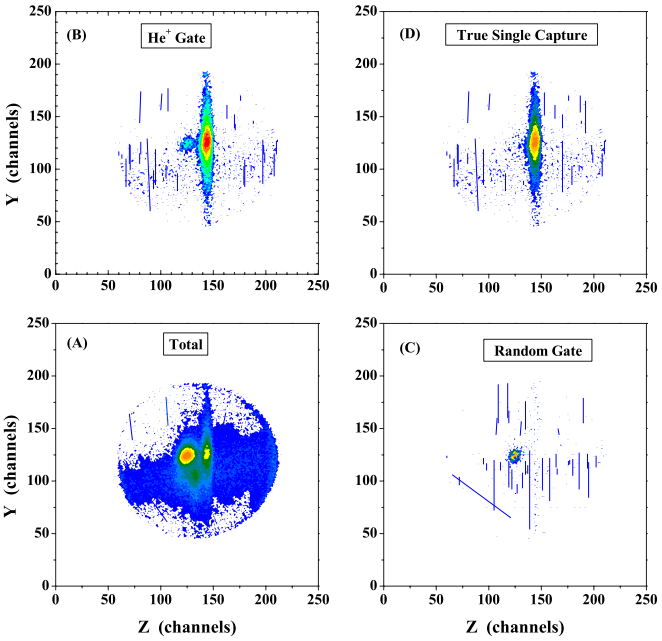

FIG. 2. (Color online) 1.5 MeV/u F^{5+}+He data recorded in coincidence with F^{4+}. (a) 2D position spectrum of all He ions. (b) 2D position spectrum gated by the He^{+} peak in the TOF spectrum. (c) 2D position spectrum gated by the random background in the TOF spectrum. (d) 2D spectrum resulting from the subtraction of (c) from (b) after proper normalization.

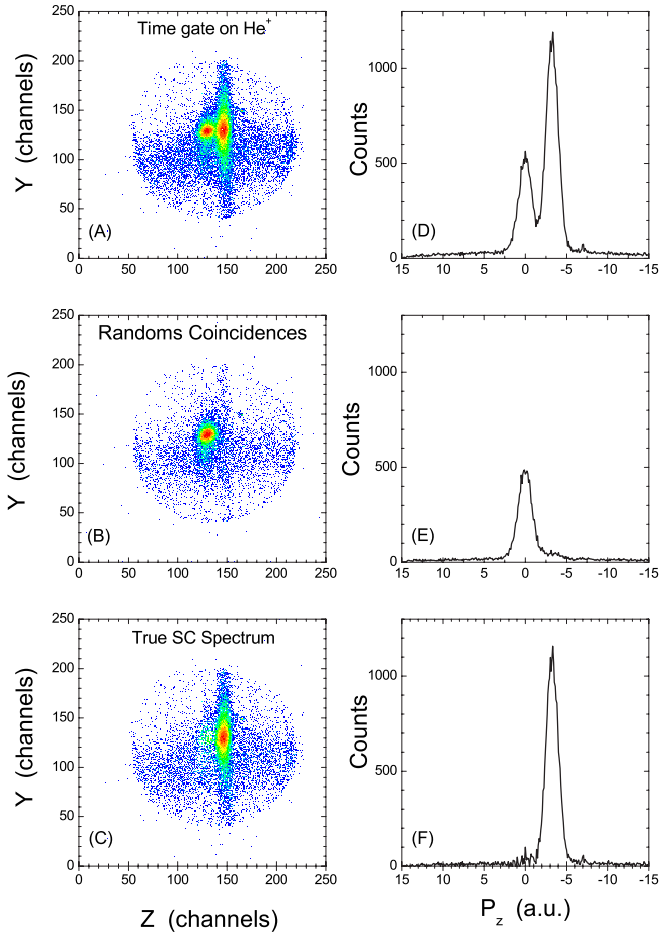

FIG. 3. (Color online) Recoil ion momentum spectra from 1 MeV/u O^{5+}+He collisions recorded in coincidence with O^{4+}. (a) All counts within the He^+ peak in the TOF spectrum, (b) random coincidences, and (c) net counts resulting from subtracting panel (b) from panel (a) after proper normalization. The corresponding panels on the right are downward projections of the respective panels on the left. They show the extracted recoil ion momentum component in the beam direction (z axis), which is pointing from right to left in this figure, thus the P_z axis on the right panels is reversed to match the 2D figures.

trometer. These voltages set up fields of 66.4 V/cm and 232.8 V/cm. The projectiles emerging from the collision region were charge state analyzed by a dipole magnet that directed the charge exchange beam into a photomultiplier tube placed 3 m downstream. Only the charge exchange beam (charge $q-1$) was detected, whereas the main beam and scattered beam were blocked with a combined four-jaw slits and a 3 mm aperture. The single charge exchange ($q-1$) projectiles were measured in coincidence with the He recoil ions. A typical data set showing the He recoil ion time-of-flight (TOF) spectrum that separates the He^{2+} from the He^+ recoils is shown in Fig. 1 for 1.5 MeV/u F^{5+} ions.

Figure 2 depicts a typical recoil-ion position spectrum produced by 1.5 MeV/u F^{5+} ions on He. The spectra are for He^{q+} recoil ion—F^{4+} projectile ion coincidences. The beam direction is right to left in the figures and the direction of the supersonic jet is from bottom to top. Figure 2(a) depicts the total coincidence spectrum. The left-most peak in Fig. 2(a) is

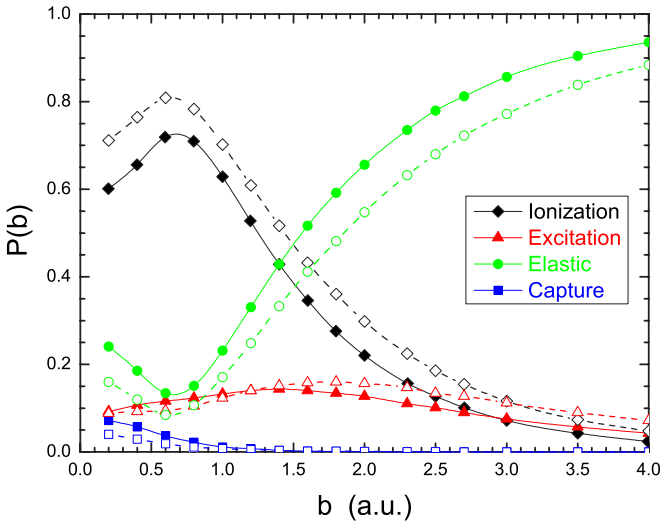

FIG. 4. (Color online) The calculated probabilities for ionization, excitation, elastic scattering, and electron capture as a function of the impact parameter. Full symbols computed by Tseng and Lin [19] using $Z_{eff}=2$, while $Z_{eff}=1.7$ was used for the open symbols (see text).

a He^+ peak associated with ionization events caused by the $F^{(q-1)+}$ contaminant charge state in the beam, i.e., coincidences between ionization events and F^{q+} ions which captured one electron either before or after crossing the jet target. The right-most peak is a He^+ peak associated with SC events. The ionization peak is at nearly zero transverse momentum whereas the SC peak can be seen to be shifted to the backward direction as expected for single electron capture to a fast moving projectile. Both peaks appear above the horizontal stripe of counts coming from the room temperature background gas. This vertical displacement is due to the velocity of the gas jet. There is a third peak below and to the right of the ionization peak which is the He^{2+} peak from TI. The position of the peak is below the He^+ peaks due to the higher velocity of a doubly charged ion compared to a singly charged ion. In other words, on average the ion hits the detector in a shorter time and does not drift as far in the vertical direction. A similar argument can be given for its horizontal position. Figures 2(b) and 2(c) depict the two-dimensional (2D) spectra as gated by the He^+ peak and as gated by a similar time width in the region of random coincidences, respectively. Figure 2(d) depicts the true single electron capture spectra which is the result of subtracting the random from the He^+ gated spectra.

A similar set of 2D data and figures can be obtained for the TI process by placing a gate on the He^{2+} peak in the TOF spectrum, a gate on an equal time window on the random events, and then subtracting the two in order to obtain the true TI yield.

The left column of graphs in Fig. 3 depicts a similar set of data for 1 MeV/u O^{5+} on He and contains the He^+ gated 2D spectrum [Fig. 3(a)] the random spectrum [Fig. 3(b)], and the true SC spectrum [Fig. 3(c)]. The graphs on the right column are the corresponding downward projections of the yields onto the horizontal axis (z axis). Gates can be placed on the y axis to better define a background-free yield. The z position

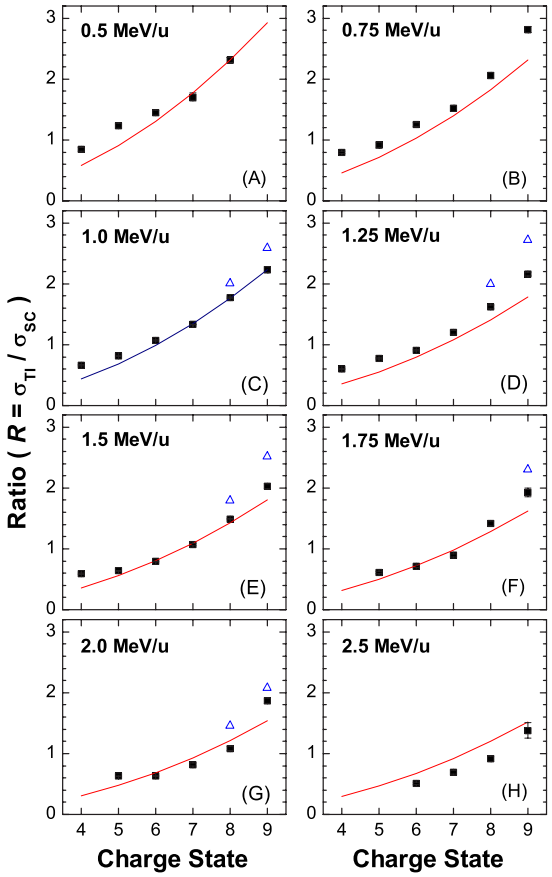

FIG. 5. (Color online) The measured ratio of transfer ionization to single capture for 0.5–2.5 MeV/u F^{q+} (q=4+ to 9+)—solid squares. The solid lines represent a q^2 scaling normalized to previous He^{2+}+He data [4]. The open triangles for F^{9+} and F^{8+} are theoretical values from Tseng and Lin calculations [19]. The error bars in the present data are purely statistical.

is, then, converted to the z component of momentum in atomic units using the measured time of flight of the recoil ions, and taking into account the ion trajectories due to the applied voltages and the geometry of the recoil ion spectrometer (further details are provided in Ref. [17]). The z component of momentum can then be used to obtain the Q value of the reaction, Q, by the relation $P_z v_p = Q + v_p^2/2$, where v_p is the projectile velocity [18]. Figure 3(f) shows a clearly separated peak corresponding to the pure single electron capture process with a momentum of about −3 a.u. This result indicates that for this case capture is primarily to the n=3 states of O^{4+}.

TABLE I. The TI to SC ratios predicted by the TCAO calculations for F^{9+} on He collision systems.

Theoretical calculation	Charge state	Energy (MeV/u)			
		1.0	1.25	1.5	2.0
Shingal and Lin [20]	9	1.75		1.1	0.86
Tseng and Lin [19]	9	2.59	2.73	2.52	2.08
	8	2.01	1.99	1.80	1.45

III. TWO CENTER ATOMIC ORBITAL CALCULATIONS

Two center atomic orbital (TCAO) close coupling calculations of the ionization, excitation, elastic scattering, and electron capture probabilities as a function of impact parameter, b, conducted by Tseng and Lin [19] for 1 MeV/u F^{9+} on He, are presented in Fig. 4. In these calculations, the independent electron model is used. Each electron in He is assumed to be in an effective Coulomb potential, $V=-Z_{eff}/r$, with an effective charge, Z_{eff}=1.7, such that the binding energy of each electron is half of the double ionization energy of He. A basis set consisting of 40 atomic states (s, p, d, and f) on the projectile ($F^{(9-8)+}$) and 103 atomic states (s, p, d, and f) on the target helium (He^+) was used to study the collisions between the F^{q+} projectiles and He for impact energies of 1, 1.25, 1.5, and 2.0 MeV/u. Bound and positive energy pseudostates in addition to the exact n=1–5 states of He^+ are included in the basis set. Table I gives the results of the TCAO calculations for F^{9+} on He collision systems. For comparison the published calculations of Shingal and Lin [20] are included.

We see from the plots in Fig. 4 that $P_i(b)$ is indeed approximately constant over the impact parameter range, where the capture probability, $P_c(b)$, has significant contributions. Furthermore, $P_c(b)$ fulfills the conditions assumed in the

TABLE II. The observed ratio of transfer ionization to single capture for F^{q+} incident on He.

Energy (MeV/u)	Projectile charge state					
	4	5	6	7	8	9
0.5	0.85±0.03	1.23±0.04	1.45±0.04	1.71±0.07	2.31±0.05	
0.75	0.80±0.02	0.92±0.05	1.26±0.03	1.52±0.05	2.06±0.01	2.81±0.05
1.0	0.66±0.01	0.82±0.01	1.07±0.01	1.33±0.01	1.77±0.01	2.23±0.05
1.25	0.61±0.01	0.78±0.01	0.91±0.01	1.20±0.03	1.62±0.03	2.16±0.03
1.5	0.59±0.01	0.64±0.01	0.79±0.01	1.07±0.02	1.49±0.01	2.03±0.04
1.75		0.62±0.02	0.71±0.02	0.89±0.03	1.42±0.04	1.92±0.07
2.0		0.63±0.01	0.63±0.01	0.82±0.03	1.08±0.04	1.87±0.05
2.5			0.51±0.02	0.69±0.05	0.91±0.05	1.38±0.13

TABLE III. Measured cross sections for one-electron transfer, single capture, and transfer ionization for (a) F^{8+} and (b) F^{9+} incident on He. All one electron-transfer cross sections are from Dillingham *et al.* [22]. The columns "Expt." give the deduced cross sections (see text) in units of 10^{-18} cm^2. The measured cross sections are also compared to theory, i.e, coupled-channels calculations of Tseng and Lin [19].

	Energy/u	$\sigma_{8,7}$	$\sigma_{8,7}^{0,1}$		$\sigma_{8,7}^{0,2}$	
	(MeV/u)	Ref. [22]	Expt.	Theory	Expt.	Theory
(a)	0.50	80	24.1		55.8	
	0.75	12.5	4.09		8.41	
	1.00	3.37	1.22	1.17	2.15	2.34
	1.25	1.57	0.60	0.47	0.971	0.93
	1.50	0.67	0.27	0.20	0.399	0.37
	1.75	0.38	0.16		0.223	
	2.00	0.15	0.072	0.056	0.078	0.082
	2.50	0.085	0.044		0.041	
	Energy/u	$\sigma_{9,8}$	$\sigma_{9,8}^{0,1}$		$\sigma_{9,8}^{0,2}$	
	(MeV/u)	Ref. [22]	Expt.	Theory	Expt.	Theory
(b)	0.75	13	3.41		9.59	
	1.00	5.26	1.63	1.25	3.63	3.24
	1.25	2.20	0.70	0.49	1.50	1.33
	1.50	1.00	0.33	0.22	0.67	0.55
	1.75	0.50	0.17		0.33	
	2.00	0.28	0.098	0.061	0.18	0.13
	2.50	0.14	0.059		0.081	

derivation of Eq. (4). If we consider the value $P_i \sim 0.7$ as given in Fig. 4 for $b<1$ a.u. and use Eq. (4), one can easily calculate the TI to SC ratio to be ~ 2.5. The ratio obtained by this simple method is in close agreement with the full calculation which gives $R=2.59$.

The value of $P_i(b)$ scales as the square of the projectile charge (i.e., q^2) in first order perturbation theory. It is therefore expected from Eq. (4) that the TI to SC ratio is $R \propto q^2$. The TI to SC ratio for 1 MeV/u He^{2+}+He has been measured to be 0.11 ± 0.02 [4]. The q^2 scaling then predicts the ratio for 1 MeV/u F^{9+}+He to be 2.23, which agrees with the result of 2.5 obtained above. Therefore, even with $P_i(b)$ values as large as 0.7, as in the F^{9+} case, the q^2 dependence seems to hold. For larger values of q or slower collisions, the approximation $P_i \propto q^2$ breaks down because the collision is no longer in the perturbative regime. One can easily imagine that $P_i(b)$ saturates at 1 for these larger values of q. This study aims to determine the q dependence experimentally for collision velocities between 4.5 and 10 a.u.

IV. RESULTS AND DISCUSSION

A. Ratios of TI to SC cross sections

Figure 5 shows the measured transfer ionization to single capture ratio obtained for 0.5–2.5 MeV/u F^{q+}+He collisions. Our study includes both dressed and bare fluorine projectiles. The target is well localized in our measurements, therefore we have not suffered from the problems and corrections that occurred in previous gas cell experiments [24,25]. Furthermore, the use of momentum transfer to separate the single capture channel from the ionization of the He target by the contaminant $F^{(q-1)+}$ beam helps reduce such systematic errors dramatically, thus resulting in high accuracy TI to SC ratios.

The data included in Fig. 5 are 0.5 MeV/u to 2.5 MeV/u $F^{(4-9)+}$ ions incident on He with three exceptions: measurements for 0.5 MeV/u F^{9+} on He could not be made because of the very low projectile-beam current, and measurements for 2.0 MeV/u F^{4+} and 2.5 MeV/u F^{5+} could not be made due to the fact that the dipole magnet was not powerful enough to bend the charge-exchanged F^{3+} and F^{4+} beams, respectively. All other charge states at all energies were measured. In all runs, TI and SC peaks were clearly separated from any contamination contribution. For F^{q+} ions incident on He, the ratio of transfer ionization to single capture is given in Table II.

We compared our measurements with calculations done by Shingal and Lin [20] and Tseng and Lin [19] for bare and hydrogenlike projectiles. Unfortunately, calculations for $F^{(4-7)+}$ on He are not available to date. Also, the q^2 dependence is plotted for all the data. Even though it is not expected that the data will follow the q^2 dependence when R becomes large, it is used as a "reference guide" to the trend in the data. The q^2 dependence is normalized to the He^{2+}+He published data [4].

Figure 5(c), for example, shows a plot of the σ_{TI}/σ_{SC} ratios as a function of projectile charge q for 1 MeV/u

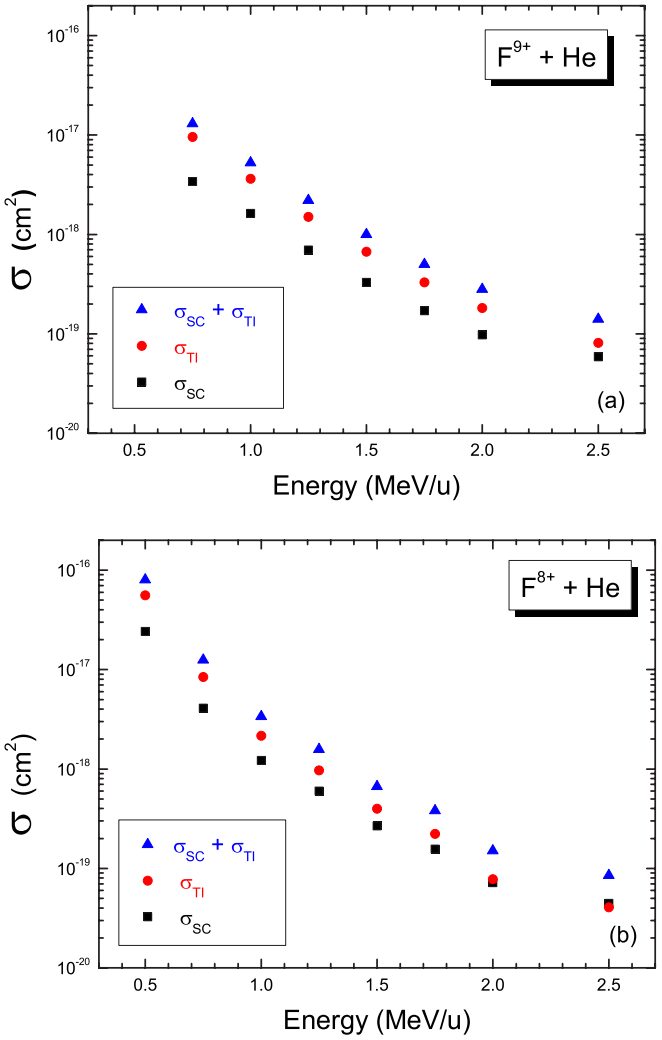

FIG. 6. (Color online) The measured cross sections for total one-electron transfer [22], single electron capture (SC), and transfer ionization (TI) for (a) F^{9+}+He and (b) F^{8+}+He. The latter two cross sections are deduced from the present measured values of R and total one-electron transfer [22].

$F^{(4-9)+}$ on He. The solid line represents a q^2 scaling normalized to He^{2+}+He. The bare F^{9+}, hydrogenlike F^{8+}, and F^{7+} ratios scale extremely well with q^2 dependence normalized to the 1 MeV/u He^{2+}+He data. Furthermore, it is reasonable that the He^{2+} sees full screening for the tightly bound K-shell structure of F^{8+} and F^{7+} projectiles. The calculations of Tseng and Lin [19] are displayed also. The calculated q dependence matches the data but is slightly larger than the measured ratio. We may conclude that these collisions can be approximately described within the perturbative regime. The data for F^{4+}, F^{5+}, and partly F^{6+} demonstrate the effect of dressing the projectile. This antiscreening effect takes place because ionization in the TI process occurs within the projectile electron cloud and increases the effective charge and therefore enhances the ionization cross section. Deviations from the q^2-scaled ratio can also arise from the behavior of the capture probability; however, this probability is usually small for these systems as can be seen in the calculations of Tseng and Lin [19] that are given in Fig. 4.

The trend seen in the 1 MeV/u data is characteristic of the data at other energies. The 0.5 MeV/u data in Fig. 5(a) is a good example. The F^{8+} and F^{7+} data agree extremely well with scaled He^{2+}+He data, whereas the lower charge states do not due to antiscreening. The highest energy data, 2 MeV/u, for F^{9+}, also agrees very well with q^2-scaled He^{2+}+He data for F^{9+} but shows a behavior for the other charge states that cannot be explained by the simple screening model. Overall, the q^2 scaling is in reasonable agreement with the data over a wide range of projectile charge states and impact energies, suggesting that it can be used to estimate the cross sections even though it is a result of a simple approximation.

B. Total SC and TI cross sections

The single capture and transfer ionization cross sections can be calculated from the presently measured TI to SC cross-section ratio, R, and the total one-electron transfer cross sections $\sigma_{q,q-1}=\sigma_{SC}+\sigma_{TI}$, provided from previous studies [22] by using the following relations:

$$\sigma_{SC} \equiv \sigma_{q,q-1}^{01} = \sigma_{q,q-1}\frac{1}{1+R}, \tag{5}$$

$$\sigma_{TI} \equiv \sigma_{q,q-1}^{02} = \sigma_{q,q-1}\frac{R}{1+R}. \tag{6}$$

The measured cross sections for total one-electron transfer, $\sigma_{q,q-1}$, for F^{8+} and F^{9+} ions incident on He are available in the literature [21–23]. The single capture and transfer ionization cross sections are calculated using Eqs. (5) and (6), our measured values of R, and the cross sections from Dillingham *et al.* [22]. The results are given in Table III for F^{8+} and F^{9+}. These results are also depicted in Figs. 6(a) and 6(b) for F^{9+} and F^{8+}, respectively. Present results agree well with Shinpaugh *et al.* [24] for the TI cross sections, but differ for the single electron capture process. Shinpaugh *et al.* [24] performed the experiments in a differentially pumped gas cell and calculated corrections to the background contributions. In these experiments it was difficult to correct for the contaminant charge beam causing ionization of He and thus appearing as a TI event. Corrections between 10% and 50% and uncertainties in the values of SC between 10% to 40% were reported [21].

V. CONCLUSION

A systematic study of the transfer ionization to single capture ratios as a function of projectile charge and speed was presented. The measured ratios are higher than those reported previously by Wu *et al.* [23] and Shinpaugh *et al.* [21], mainly because of the improved separation of the pure single capture from the ionization by the $F^{(q-1)+}$ contaminant beam. This improvement is due to a better localized target and the application of momentum imaging which allowed us to separate ionization from capture by their different longitudinal momentum, thus providing high accuracy ratios. Total SC and TI cross sections were evaluated using our mea-

sured ratios and previously reported total single electron transfer cross sections [22].

The collision systems reported here are 0.5–2.5 MeV/u (i.e., v_p=4.5 to 10 a.u.) $F^{(4-9)+}$ ions interacting with helium. The TI to SC ratios monotonically decrease with increasing collision energy. Furthermore, the ratios increase with projectile charge roughly following the q^2 scaling expected for ionization in the perturbative regime. This indicates that capture occurs preferentially over a small range of impact parameters where the ionization probability is approximately constant as indicated by the simple independent electron approximation. The data are also in reasonable agreement with coupled-channel calculations where both show the same dependence on projectile energy. However, the data are systematically lower than the theoretical predictions.

ACKNOWLEDGMENTS

The authors wish to thank Professor Kevin Carnes for helpful comments. This work was supported by the Chemical Sciences, Geosciences, and Biosciences Division, Office of Basic Energy Sciences, Office of Science, U.S. Department of Energy.

[1] G. H. Henderson, Proc. R. Soc. London, Ser. A **102**, 496 (1922).
[2] A. S. Schlachter, J. W. Stearns, W. G. Graham, K. H. Berkner, R. V. Pyle, and J. A. Tanis, Phys. Rev. A **27**, 3372 (1983).
[3] H. Knudsen, H. K. Haugen, and P. Hvelplund, Phys. Rev. A **23**, 597 (1981).
[4] H. Knudsen, L. H. Andersen, P. Hvelplund, J. Sorensen, and D. Ciric, J. Phys. B **20**, L253 (1987).
[5] R. Bartiromo, in *Diagnostics for Fusion Reactor Condition*, Proceedings of the International School of Plasma Physics, edited by P. E. Stott, D. K. Akulina, G. G. Leota, E. Sindoni, and C. Wharton (Pergamon, New York, 1982).
[6] G. Steigman, Astrophys. J. **199**, 642 (1975).
[7] H. S. W. Massey and E. H. S. Burhop, *Electronic and Ionic Impact Phenomena* (Clarendon Press, Oxford, 1952).
[8] S. K. Allison, Rev. Mod. Phys. **30**, 1137 (1958).
[9] S. K. Allison and M. Garcia-Munoz, in *Atomic and Molecular Process*, edited by D. R. Bates (Academic Press, New York, 1962).
[10] J. B. Hasted, *Physics of Atomic Collisions* (Butterworth, London, 1964).
[11] H.-D. Betz, Rev. Mod. Phys. **44**, 465 (1972).
[12] H. Tawara and A. Russek, Rev. Mod. Phys. **45**, 178 (1973).
[13] H. S. W. Massey and H. B. Gilbody, *Electronic and Ionic Impact Phenomena* (Clarendon Press, Oxford, 1974), Vol. 4.
[14] H. B. Gilbody, Adv. At. Mol. Phys. **22**, 143 (1986).
[15] B. H. Bransden and M. R. C. McDowell, *Charge Exchange and the Theory of Ion Atom Collisions* (Oxford University Press, New York, 1992).
[16] R. Ünal, P. Richard, H. Aliabadi, H. Tawara, C. L. Cocke, I. Ben-Itzhak, M. J. Singh, and A. T. Hasan, *Application of Accelerators in Research and Industry*, edited by J. L. Duggan and I. L. Morgan (AIP Press, New York, 2001), Vol. 576, p. 36.
[17] R. Ünal, Ph.D. thesis, Kansas State University, 2001 (electronic version available at http://jrm.phys.ksu.edu/publications.html).
[18] V. Frohne, S. Cheng, R. Ali, M. L. A. Raphaelian, C. L. Cocke, and R. E. Olson, Phys. Rev. Lett. **71**, 696 (1993).
[19] H. C. Tseng and C. D. Lin (private communication).
[20] R. Shingal and C. D. Lin, J. Phys. B **24**, 251 (1991).
[21] J. L. Shinpaugh, J. M. Sanders, J. M. Hall, D. H. Lee, H. Schmidt-Böcking, T. N. Tipping, T. J. M. Zouros, and P. Richard, Phys. Rev. A **45**, 2922 (1992).
[22] T. R. Dillingham, J. R. Macdonald, and P. Richard, Phys. Rev. A **24**, 1237 (1981).
[23] W. Wu, Ph.D. thesis, Kansas State University, 1994.
[24] V. V. Afrosimov, A. A. Basalaev, E. D. Donets, K. O. Lozhkin, and M. N. Panov, in *Abstracts of the 12th International Conference on the Physics of Electronic and Atomic Collisions*, edited by S. Datz (North Holland, Amsterdam, 1982), p. 690.
[25] E. Horsdal Pederson and L. Larsen, J. Phys. B **12**, 4085 (1979).